Development of a Global Infrared Land Surface Emissivity Database for Application to Clear Sky Sounding Retrievals from Multispectral Satellite Radiance Measurements

SUZANNE W. SEEMANN, EVA E. BORBAS, ROBERT O. KNUTESON, GORDON R. STEPHENSON,* AND HUNG-LUNG HUANG

Cooperative Institute for Meteorological Satellite Studies, University of Wisconsin—Madison, Madison, Wisconsin

(Manuscript received 14 September 2006, in final form 20 March 2007)

ABSTRACT

A global database of infrared (IR) land surface emissivity is introduced to support more accurate retrievals of atmospheric properties such as temperature and moisture profiles from multispectral satellite radiance measurements. Emissivity is derived using input from the Moderate Resolution Imaging Spectroradiometer (MODIS) operational land surface emissivity product (MOD11). The baseline fit method, based on a conceptual model developed from laboratory measurements of surface emissivity, is applied to fill in the spectral gaps between the six emissivity wavelengths available in MOD11. The six available MOD11 wavelengths span only three spectral regions (3.8–4, 8.6, and 11–12 μm), while the retrievals of atmospheric temperature and moisture from satellite IR sounder radiances require surface emissivity at higher spectral resolution. Emissivity in the database presented here is available globally at 10 wavelengths (3.6, 4.3, 5.0, 5.8, 7.6, 8.3, 9.3, 10.8, 12.1, and 14.3 μm) with 0.05° spatial resolution. The wavelengths in the database were chosen as hinge points to capture as much of the shape of the higher-resolution emissivity spectra as possible between 3.6 and 14.3 μm. The surface emissivity from this database is applied to the IR regression retrieval of atmospheric moisture profiles using radiances from MODIS, and improvement is shown over retrievals made with the typical assumption of constant emissivity.

1. Introduction

The operational algorithm for retrieving temperature and moisture profiles and total column ozone from infrared (IR) radiances observed by the National Aeronautics and Space Administration Earth Observing System (NASA EOS) Moderate Resolution Imaging Spectroradiometer (MODIS) instrument is a clear sky synthetic regression retrieval algorithm called MOD07 (Seemann et al. 2003, 2006). Atmospheric retrieval algorithms such as MOD07 require a global set of profiles and corresponding surface data (surface emissivity, surface skin temperature, and surface pressure) to train the synthetic regression. Radiance calculations for each training profile and surface values are made using a transmittance model, and the calculated radiance/atmospheric profile pairs are then used to derive the regression relationship. The MOD07 algorithm uses 11 IR channels with wavelengths from 4.5 (MODIS band 25) to 14.2 μm (MODIS band 36), and radiance calculations for these bands are made with the prototype Community Radiative Transfer Model (prototype-CRTM; Kleespies et al. 2004).

Datasets of temperature and moisture profiles for training a regression can be derived from radiosonde observations or atmospheric models. Four commonly used training databases are the National Oceanic and Atmospheric Administration-88 (NOAA-88; see online at http://cimss.ssec.wisc.edu/itwg/groups/rtwg/profiles.html), Thermodynamic Initial Guess Retrieval-3 (TIGR-3; Chedin et al. 1985), European Centre for Medium-Range Weather Forecasts (ECMWF; Chevallier 2001), and SeeBor (Borbas et al. 2005) training databases. The MOD07 regression coefficients are derived from the SeeBor training database of global profiles, which consists of 15 704 global profiles of temperature, moisture, and ozone at 101 pressure levels for clear sky conditions.

The NOAA-88, TIGR-3, and ECMWF training da-

* Current affiliation: Scripps Institution of Oceanography, University of California, San Diego, La Jolla, California.

Corresponding author address: Suzanne W. Seemann, CIMSS/UW-Madison, 1225 W. Dayton St., Madison, WI 53716.
E-mail: suzanne.seemann@ssec.wisc.edu

DOI: 10.1175/2007JAMC1590.1

TABLE 1. MODIS IR channels between 3.8 and 14.2 μm. Channels used in the MOD07 retrieval algorithm and channels for which emissivity is available in the MOD11 algorithm are indicated with an X.

MODIS IR channels	20	22	23	25	27	28	29	30	31	32	33	34	35	36
Wavelength (μm)	3.8	3.9	4.0	4.5	6.7	7.3	8.6	9.7	11.0	12.0	13.3	13.6	13.9	14.2
Channels in MOD07				X	X	X	X	X	X	X	X	X	X	X
Channels with emissivity in MOD11	X	X	X				X		X	X				

tabases do not include emissivity estimates, and users must assign emissivity values at the wavelengths that correspond to the channels used in the retrievals for each profile. While each profile would ideally have an actual observed emissivity collocated in time and space for all wavelengths, emissivity measurements with sufficiently high spectral resolution are performed only in the laboratory or in limited regions for field campaigns. It is therefore not possible to go back and assign a measured emissivity collocated in time and space for all MODIS IR wavelengths to the globally distributed historic profiles. As a result, the training databases used for retrieval algorithms typically include a highly approximate surface characterization for each profile.

This paper presents a global database of IR land surface emissivity with high spatial, moderate spectral, and monthly temporal resolution suitable for use in synthetic regression retrievals of atmospheric profiles. This piecewise linear application is best suited for multispectral, filter instruments such as MODIS, Geostationary Operational Environmental Satellite (GOES), Spinning Enhanced Visible and Infrared Imager (SEVIRI), and High Resolution Infrared Radiation Sounder (HIRS), and is not intended for high–spectral resolution instruments such as Atmospheric Infrared Sounder (AIRS) and Geosynchronous Imaging Fourier Transform Spectrometer (GIFTS), where more detailed spectral emissivity information is required. Emissivity was derived using a procedure that fills in the spectral gaps between operational MODIS land surface emissivity product (MOD11) wavelengths by fitting monthly averaged MOD11 land surface emissivity values to a baseline emissivity spectrum. The result is called the baseline fit (BF) emissivity database. This database will improve the accuracy of atmospheric parameters retrieved using an IR synthetic retrieval algorithm by providing land surface emissivity values for every wavelength used in the regression.

Background on the emissivity measurements used in this paper is presented in section 2. The derivation of the BF global land surface emissivity database is described in section 3. Improvements to MOD07 retrievals of total precipitable water vapor over land after application of the emissivity to the training data are demonstrated in section 4. Conclusions and projections for future work are provided in section 5.

2. Background

a. Emissivity in regression retrieval algorithms

Previous work to derive a global surface emissivity database has been directed toward the calculation of the surface radiation budget for applications to climate studies (Zhou et al. 2003; Ogawa and Schmugge 2004). Because these efforts involve a broadband emissivity, they are not applicable for atmospheric property retrievals. Surface emissivity derived from satellite radiances is available globally, but not at high enough spectral resolution for these retrievals. For example, MOD11 (Wan and Li 1997; Wan 1999) includes emissivity for only three of the eleven MODIS bands needed by the MOD07 algorithm, as shown in Table 1.

Kornfield and Susskind (1977) conducted sensitivity analyses for the HIRS and Vertical Temperature Profile Radiometer (VTPR) instruments and demonstrated that an accurate surface emissivity is critical for the retrievals of surface temperature and temperature profiles. However, without a realistic multispectral global database of surface emissivity, constant value or random surface emissivity spectra are still common. The Visible and IR Spin-Scan Radiometer Atmospheric Sounder (VAS), for example, used a constant emissivity of 0.96 over land and 1.0 over water (Hayden 1988). Other algorithms, including earlier MODIS retrievals (Seemann et al. 2003) and retrievals from the Advanced Television Infrared Observation Satellite (TIROS) Operational Vertical Sounder (ATOVS; Li et al. 2000) assigned the emissivity randomly with a given standard deviation. The emissivity assigned to profiles in the NOAA-88 training database used with the earlier operational MODIS and ATOVS atmospheric retrievals is illustrated in Fig. 1. For comparison, laboratory-measured emissivity spectra of some common materials are also shown. The range of spectra assigned to the ATOVS and early MODIS training data shown in Fig. 1 do not capture the reduction in emissivity in the 8–10-μm region, which is important for characterizing certain surface materials, particularly quartz in sandy soils.

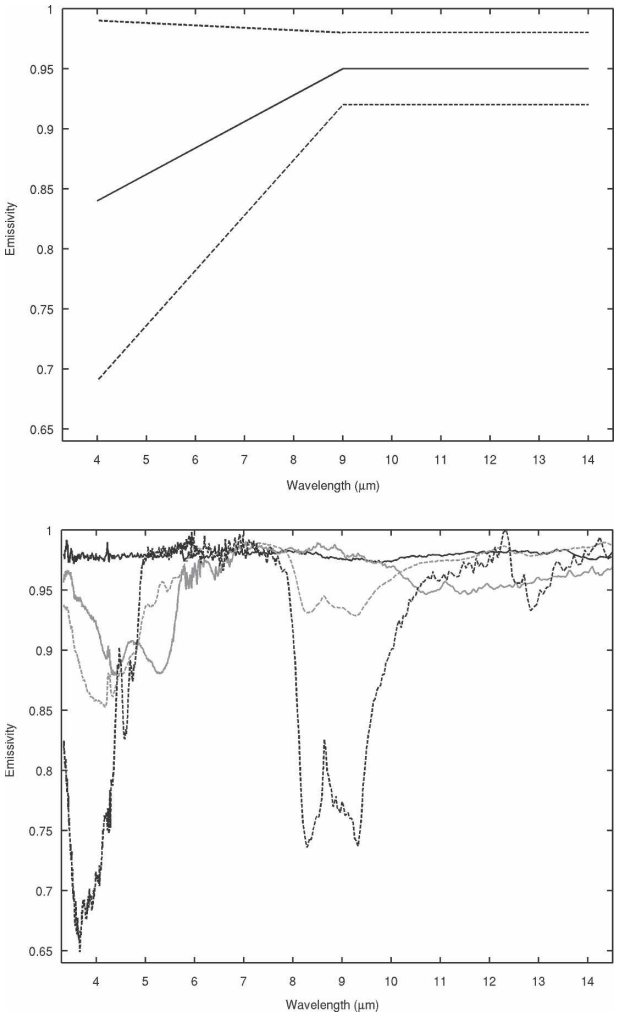

FIG. 1. (top) Mean (solid) and ±1 std dev (dashed) for emissivity assigned to the NOAA-88 training data profiles in the ATOVS and early MODIS atmospheric retrieval algorithms compared with (bottom) laboratory-measured surface emissivity spectra for selected land surface types. Spectra shown are for pine (solid black), dry grass (solid gray), Concord, MA, soil (dashed gray), and sandy soil from Page (dashed black). Laboratory data shown here were drawn from the University of California, Santa Barbara, emissivity library (http://www.icess.ucsb.edu/modis/EMIS/html/em.html).

In addition, the laboratory-derived pine and grass spectra do not have the variation in emissivity at 4 μm, which is inherent to the random model. By randomly applying the emissivity in this manner, without regard to ecosystem type or geographical location, an evergreen forest could be assigned a spectrum with an emissivity value of 0.7 at 4 μm, and a desert scene could have a near-constant emissivity at 0.98 for all wavelengths. As shown in this paper, such inaccuracies in the emissivities assigned to training data profiles can have a significant effect on atmospheric moisture retrievals.

b. *Emissivity measurements*

Approaches for retrieving surface temperature and emissivity from satellite data include the day/night approach used by the NASA MODIS land team, the split-window approach also used by MODIS, and the temperature and emissivity separation (TES) method used by the Advanced Spaceborne Thermal Emission and Reflection Radiometer (ASTER) instrument (Dozier and Wan 1994; Wan and Li 1997; Wan 1999; Gillespie et al. 1999). These approaches have their particular strengths and weaknesses depending on the type of surface for which the retrieval is made as well as the characteristics of the available satellite data and intermediary atmosphere. The day–night approach applied by the MOD11 product used in this paper assumes that emissivity does not change between day and night views of the same location over the period of a few days (Wan and Li 1997; Wan 1999). Surface emissivity in the MOD11 product is only retrieved in the six bands where the earth's surface can make significant contributions to the thermal IR signals received by MODIS. These bands (20, 22, 23, 29, 31, and 32) are positioned within the 3.5–4.2- and 8–13-μm atmospheric windows. Although the 9.7-μm MODIS band 30 lies within a window, it was omitted because of strong ozone absorption at this wavelength (Wan and Li 1997).

The MOD11 products are generated operationally for all clear sky scenes (both day and night) over land by the NASA MODIS Data Processing System (MODAPS) and are distributed by Land Processes Distributed Active Archive Center (LP DAAC) for every 5-min MODIS granule on both the NASA EOS *Terra* and *Aqua* satellites. (The products derived from the *Aqua* radiances are termed MYD11.) These granules are also averaged down to daily, eight-day, and monthly products. For the present study, monthly averages were used. The same procedure could be repeated for a shorter averaging period, thereby increasing the temporal resolution of the database. However, as the averaging time is reduced, more cloudy pixels will limit the coverage of MOD11 data.

In addition to satellite measurements of emissivity, the IR reflectivities of materials have been measured in the laboratory, and these laboratory measurements have been complemented with ground- and aircraft-based measurements of natural surfaces (Salisbury and D'Aria 1992 1994; Korb et al. 1996; Knuteson et al. 2004; Hook et al. 2005). The laboratory measurements used in the derivation of the emissivity in this paper were drawn from the MODIS emissivity library (http://www.icess.ucsb.edu/modis/EMIS/html/em.html) and the ASTER spectral library (Salisbury et al. 1994). The

two datasets include spectra of natural and manmade materials. The MODIS emissivity library data were measured by the Institute for Computational Earth System Science at the University of California, Santa Barbara (ICESS/UCSB). The ASTER spectral library includes data from the Johns Hopkins University (JHU) Spectral Library, the Jet Propulsion Laboratory (JPL) Spectral Library, and the U.S. Geological Survey (USGS) Spectral Library.

3. Derivation of baseline fit land surface emissivity database

The MOD11 land surface emissivity product was chosen as the starting point for the derivation of a global land surface emissivity database. The MOD11 product has the advantage of high spatial resolution (0.05° in the monthly averaged product), although spectral resolution is limited. MOD11 includes emissivity at only 3 of the 11 bands required by the MOD07 retrieval algorithm, as illustrated in Table 1. To fill in the spectral gaps in MOD11 emissivity data, high–spectral resolution laboratory measurements of surface emissivity from the USCB and ASTER Spectral Libraries are also included in the derivation. Although these measurements have the advantage of providing high spectral resolution (wavenumber resolution between 2 and 4 cm^{-1}), such laboratory-measured materials are not true representations of a global ecosystem as seen from space. The effects of surface structure and roughness are not included in the laboratory measurements (Snyder and Wan 1998). For example, a single pine needle or a pile of needles in the laboratory may have quite different spectral properties compared to an evergreen forest canopy as seen from space. In addition, most laboratory measurements are made from individual raw materials, whereas any region of the earth's surface spanned by the satellite footprint typically consists of a combination of soils, minerals, vegetation, and water.

The key to deriving a global emissivity database lies in the combination of the high spectral measurements made in the laboratory with the moderate spectral resolution satellite observations of actual ecosystems. The BF method developed in this study uses selected laboratory measurements of emissivity to generate a baseline emissivity spectrum, and then employs MOD11 emissivity measurements to adjust the baseline spectrum based on a conceptual model of land surface emissivity spectra. This combination of laboratory measurements and satellite-derived MODIS emissivity measurements provides a database that effectively captures global variability and heterogeneity in land surfaces.

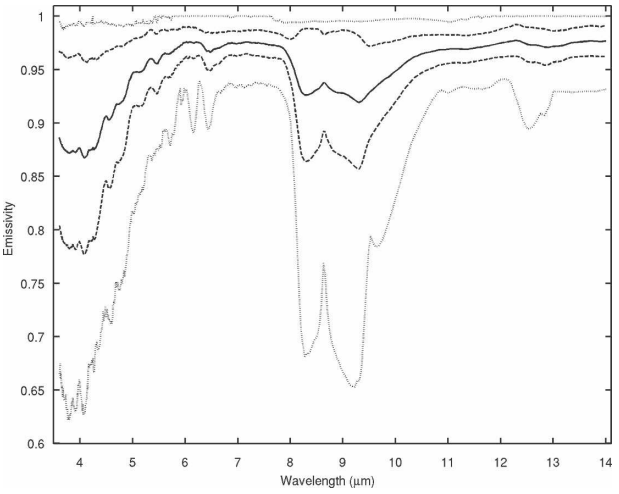

FIG. 2. Characterization of variability in 123 ICESS/UCSB land surface emissivity spectra: mean emissivity (solid), mean emissivity ±1 std dev (dashed), and maximum–minimum emissivity at each wavelength (dotted).

a. Methodology

1) CONCEPTUAL MODEL

The first step in the derivation of the BF emissivity was to screen the high–spectral resolution laboratory-measured emissivity spectra in the ICESS/UCSB emissivity library based on completeness and origin. Emissivity spectra from materials considered to be manmade or of lunar origin were excluded. Spectra were required to include the full wavelength range 3.6–14.0 μm, without data gaps. In addition, spectra with any emissivity less than 0.6 within this wavelength range were omitted to limit the analysis to natural materials present in earth's ecosystems. For this step, the ASTER spectral library was not included because it contains spectra for minerals and surface components that do not independently compose a land surface. This initial screening resulted in 123 ICESS/UCSB measurements that are representative of surfaces and soils present in global ecosystems. These materials include dry grass, river-washed stones, ice and snow, seawater, Santa Barbara sandstone, salty soil, twenty-two types of leaves and pine needles, and surface samples from Concord (Massachusetts), Lamont (Oklahoma), the Nebraska soil laboratory, Goleta Beach, and Koehn (California), Death Valley and Railroad Valley (Nevada), and Page (Arizona). A representation of the variability in these spectra is shown in Fig. 2.

From the 123 ICESS/UCSB spectra, a conceptual model was developed to describe the general behavior of a land surface emissivity spectrum, with the intent to provide an emissivity value at all MOD07 bands given

input at only the MOD11 wavelengths. This conceptual model can be summarized as below:

- Spectra typically slope up in the 4–7-μm region after the first 3 MOD11 bands (3.8–4.0 μm), with a region of steeper slope up to around 5 μm and often nearly leveling off before 6 μm.
- Many but not all spectra have a broad reduction in emissivity between 8 and 10 μm, associated with a strong absorption feature characteristic of quartz silicates (reststrahlen band; Prabhakara and Dalu 1976; Schmugge et al. 1998).
- If MOD11 emissivity at 8.6 μm is greater than 0.97, then the emissivity spectra is typically relatively uniform, often with all values higher than 0.97.
- Emissivity beyond 12 μm (the last wavelength for which MOD11 data are available) can be characterized as having a constant slope for all spectra equal to a rise of 0.01 over 3.5 μm.

2) HINGE POINT SELECTION

Certain wavelengths were designated as hinge points to capture the spectral shape defined by this conceptual model. Hinge points were selected after experimentation with various wavelengths to find the optimal combination for characterizing the 123 ICESS/UCSB land surface emissivity spectra. It was found that 10 hinge-point wavelengths provided a good balance by describing the shape of the spectra with sufficient resolution for application to an instrument like MODIS without requiring unnecessary assumptions. More hinge points would allow for more spectral detail, but more assumptions would also be necessary because MOD11 information is available at so few wavelengths. The 10 selected wavelengths (3.6, 4.3, 5.0, 5.8, 7.6, 8.3, 9.3, 10.8, 12.1, and 14.3 μm) are shown as the dotted vertical lines in Fig. 3, along with a reference laboratory emissivity spectra for a sample of sliced Santa Barbara sandstone. As shown in this figure, the hinge points span 1) the sharp rise in emissivity typical in the 4–5-μm region, 2) the lower slope and high emissivity values through the water vapor region, 3) the emission minimum associated with the quartz *reststrahlen* feature often centered around 8.6 μm, and 4) the sharp rise, then gradual trend upward through the IR window and far IR wavelengths.

The hinge-point wavelengths were each assigned an initial emissivity value based on selected laboratory emissivity, and the resulting spectrum is called the baseline emissivity spectrum (BES; Fig. 3, dashed line). The BES is intended only as an aid in visualizing the BF procedure and to illustrate the general shape of an emissivity spectrum. The magnitude of the BES is not

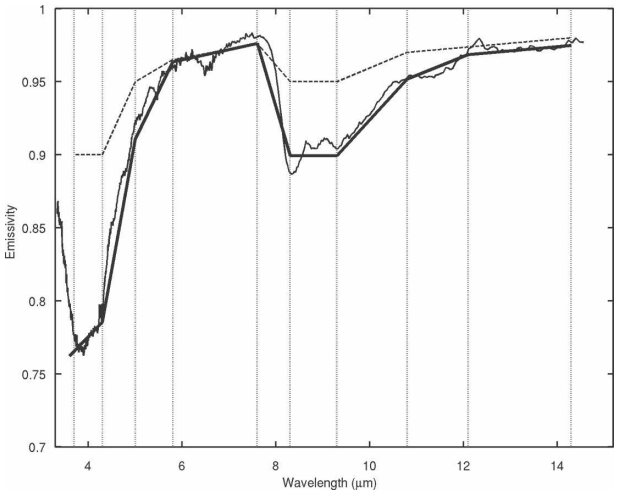

FIG. 3. Location of the hinge-point wavelengths identified by dotted vertical lines shown with surface emissivity spectra from the ICESS/UCSB emissivity library for a sample of sliced Santa Barbara sandstone (thin solid line), and the conceptual BES (dashed line). The BF emissivity spectra derived using input from the sandstone spectrum at the 6 MOD11 wavelengths are shown as the thick black line.

intended to characterize the emissivity spectra of any given land surface. Instead, the BES is adjusted at each hinge point based on the emissivity values at MOD11 wavelengths according to the fitting procedure introduced in section 3a(3). The result is a BF emissivity spectrum at 10 hinge points. This spectrum can be interpolated between hinge points to arrive at approximations of the emissivity for any wavelength between 3.6 and 14.3 μm, as shown for the Santa Barbara sandstone spectrum in Fig. 3 as the thick solid line.

3) BASELINE FIT PROCEDURE

Since the MOD11 emissivity is only available in the 3.8–4, 8.6, and 11–12-μm spectral regions, certain rules and assumptions are required in the fitting procedure to adjust the BES at the 10 hinge points. These rules were developed to apply the conceptual model outlined in 3a(1) given input at only the MOD11 wavelengths. Further, the procedure was developed through iterative testing on the subset of 123 ICESS/UCSB laboratory measurements of emissivity of general land surface materials, using input sampled at only the six MOD11 wavelengths. The fitting procedure is described below. Examples of applying the fitting procedure to MOD11 data for four selected locations with different emissivity spectral behavior are shown in Fig. 4.

1) The first step in the fitting procedure takes advantage of the 3 MOD11 emissivity values clustered in the 3.8–4.0-μm range. The slope and intercept of a

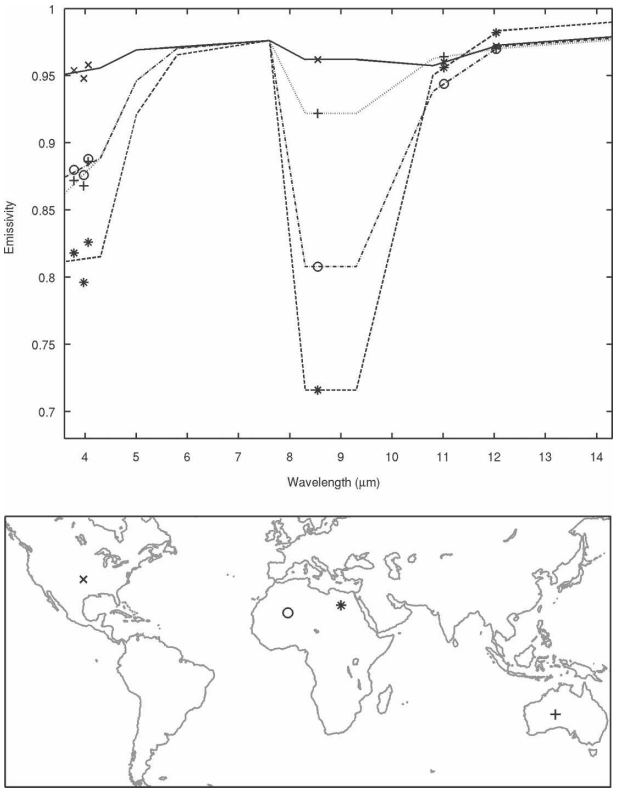

FIG. 4. (top) Examples of the application of the baseline fit procedure to MOD11 emissivity data from four sites. The six original MOD11 emissivity values are indicated by the symbols for each of the four sites: SGP ARM site in Lamont, OK (x), west-central Australia (+), eastern Sahara Desert (*), and western Sahara Desert (o). The baseline fit spectra are shown by the solid, dotted, dashed, and dashed–dotted lines, respectively. (bottom) Location of the four sites is shown in the map.

linear best fit are computed through all three values and the line is extended in both directions to span between the hinge points at 3.6 and 4.3 μm.

2) MOD11 data are not available in the 5–8-μm region where there are 3 hinge points (5.0, 5.8, and 7.6 μm). A constant emissivity value is initially assigned at wavelength 7.6 μm because there is the least variation in emissivity at this wavelength among our subset of 123 laboratory spectra. In addition, the effect of surface emissivity on radiance calculations at this wavelength is small so the impact of any errors will be minimized. A value of 0.976 was selected as the initial emissivity value at 7.6 μm based on an average over the laboratory spectra.

   Once the emissivity at 7.6 μm has been set, an initial value is assigned to the 5.0-μm hinge point so that the slope between 4.3 and 5.0 μm is greater than the slope between 5.0 and 7.6 μm, according to Eq. (1),

$$\frac{\varepsilon 4.3 - \varepsilon 5.0}{\varepsilon 5.0 - \varepsilon 7.6} = 1.9, \tag{1}$$

   where εX is the emissivity at a hinge point with wavelength X and 1.9 was computed from the ratio of the BES differences for the same wavelengths.

   After the initial emissivity values are assigned for 5.0 and 7.6 μm, additional screening is performed to determine whether an adjustment is necessary. For some materials such as grasses and leaves, emissivity is relatively constant over all wavelengths and often has a value greater than 0.976 throughout, so applying 0.976 at 7.6 μm is not appropriate. In the fitting procedure, these cases are identified by having an 8.6-μm emissivity greater than 0.97 (i.e., no emissivity dip in this region characteristic of sandy soils), and the 5.0- and 7.6-μm emissivity is computed differently. For these cases, ε5.0 is computed from Eq. (2),

$$\frac{\varepsilon 4.3 - \varepsilon 5.0}{\varepsilon 5.0 - \mathrm{M}8.6} = 1.9, \tag{2}$$

   where M8.6 is the MOD11 band 29 emissivity at 8.6 μm. Equation (2) defines ε5.0 based on the same emissivity difference ratio (1.9) introduced in Eq. (1), except the MOD11 8.6-μm value is used as the high wavelength endpoint instead of the hinge point emissivity at 7.6 μm. After calculating ε5.0 from Eq. (2) for these cases characterized by a relatively uniform emissivity, a linear fit is applied between hinge point ε5.0 and M8.6 to find ε7.6.

3) The next step for all cases is to use a linear fit between ε5.0 and ε7.6 to find an intermediary value at 5.8, called ε_L5.8, where L designates linear. For spectra that are nearly uniform in this region (defined as $\varepsilon 7.6 - \varepsilon 5.0 < 0.01$), the linear fit is used for the 5.8μm emissivity,

$$\varepsilon 5.8 = \varepsilon_L 5.8. \tag{3}$$

   For all other cases ($\varepsilon 7.6 - \varepsilon 5.0 > 0.01$), ε5.8 is computed using Eq. (4), which divides the rise in emissivity from 5.0 to 7.6 μm into 2 segments, with the segment ε5.8 – ε7.6 having a smaller slope than the ε5.0 – ε5.8 segment. This behavior is consistent with the conceptual model and is visible in the BES shown in Fig. 3,

$$\varepsilon 5.8 = \varepsilon_L 5.8 + 0.5(\varepsilon 7.6 - \varepsilon 5.0). \tag{4}$$

4) The MOD11 emissivity value at 8.6 μm is assigned to inflection points at 8.3 and 9.3 μm to span the width of a typical reduction in emissivity characteristic of the quartz silicate components of many rocks and soils in this spectral region.

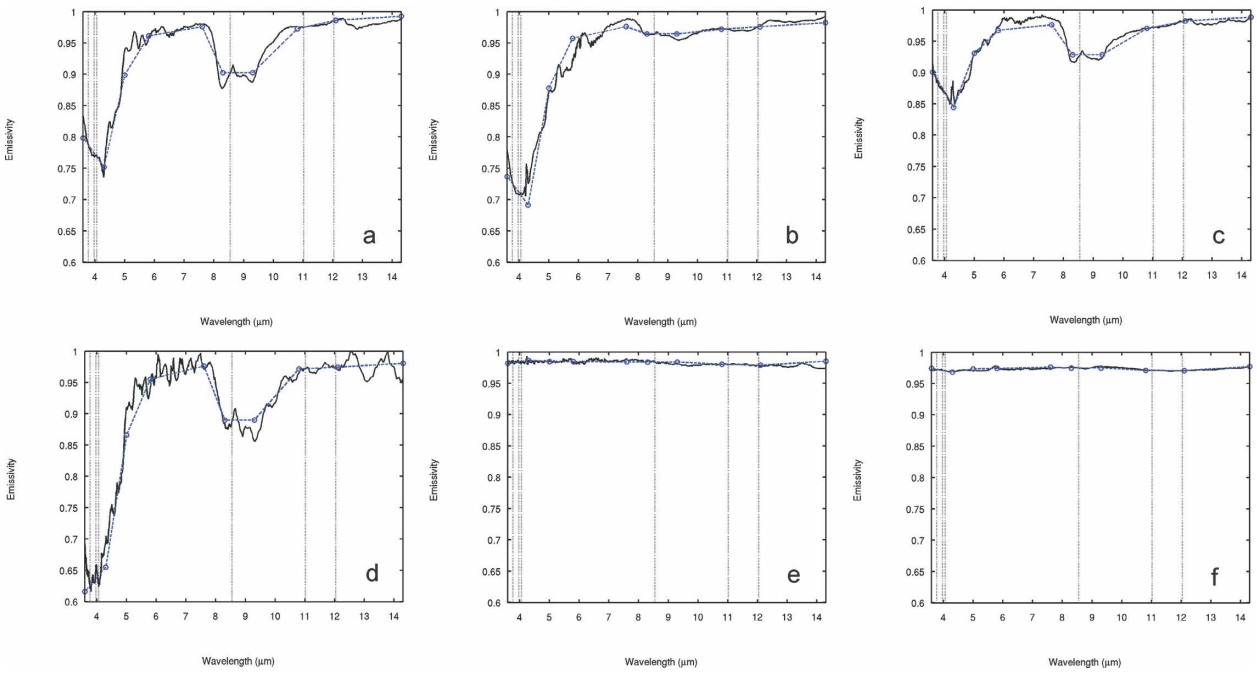

FIG. 5. Comparison of original laboratory-measured emissivity spectra as a function of wavelength (solid lines) with those derived by BF approach (dashed lines) using only the emissivity values at the MOD11 wavelengths (identified by the dotted vertical lines). Materials presented are (a) Oklahoma soil, (b) surface in Koehn, CA, (c) Concord, MA, soil, (d) soil 90p_476s from the Nebraska soil laboratory, (e) pine needles, and (f) leaves from a laurel tree.

5) For the IR window channel region, a line fit through the two MOD11 emissivity values at 11 and 12 μm is used to extend a line from hinge points 10.8–12.1 μm.
6) MOD11 data are not available in the far IR wavelengths (>12 μm). It was determined from representative laboratory data that a fixed slope of 0.0029 μm^{-1} (0.01 emissivity change over 3.5 μm) between 12.1 and 14.3 μm is suitable to find an emissivity value at 14.3 μm.

b. Evaluation of the baseline fit method

The 123 ICESS/UCSB high–spectral resolution laboratory emissivity measurements introduced in section 3a(1) were used to perform an initial evaluation of the BF procedure. (This analysis is intended to illustrate the closeness of fit in representing a full spectrum of emissivity and not to establish validation of the BF emissivity for global land surfaces.) From the high–spectral resolution laboratory data, emissivity values corresponding to the six MOD11 wavelengths were selected and input into the BF procedure outlined in section 3a(3). The result was an emissivity value at 10 hinge-point wavelengths for each of the laboratory spectra. The derived BF spectra were linearly interpolated between the 10 hinge points to arrive at a resolution of 5 cm^{-1} wavenumbers for comparison with the laboratory-measured spectra subsampled at the same wavelengths. Comparisons of the BF and original laboratory spectra for selected materials are shown in Figs. 5 and 6. For reference, the locations of the MOD11 wavelengths are indicated by the dotted vertical lines.

Although the materials in Fig. 5 have varied spectral behavior, the BF emissivity generally agrees well with the laboratory-measured emissivity in shape and magnitude. The high-spectral-resolution fluctuations in emissivity will not be captured by this approach, but they are not required for multispectral applications such as MOD07 retrievals because the MODIS instrument filter functions average over the high spectral features.

The procedure that fits the hinge-point wavelengths to MOD11 data is designed to accommodate many of the spectra that do not fit the conceptual model exactly; however, there are certain spectra that are beyond the capabilities of this model. Examples of materials that were not as well modeled by the BF approach are presented in Fig. 6 to illustrate some of its limitations. Figure 6a shows the spectrum of a soil sample collected from Page, Arizona, which contains a relatively uniform emissivity at wavelengths from 5 to 7.5 μm. Because the BF conceptual model expects a more gradual rise through this region, emissivity for this surface is underestimated in the 5–6-μm region. In addition, the laboratory-measured emissivity spectrum for the Page

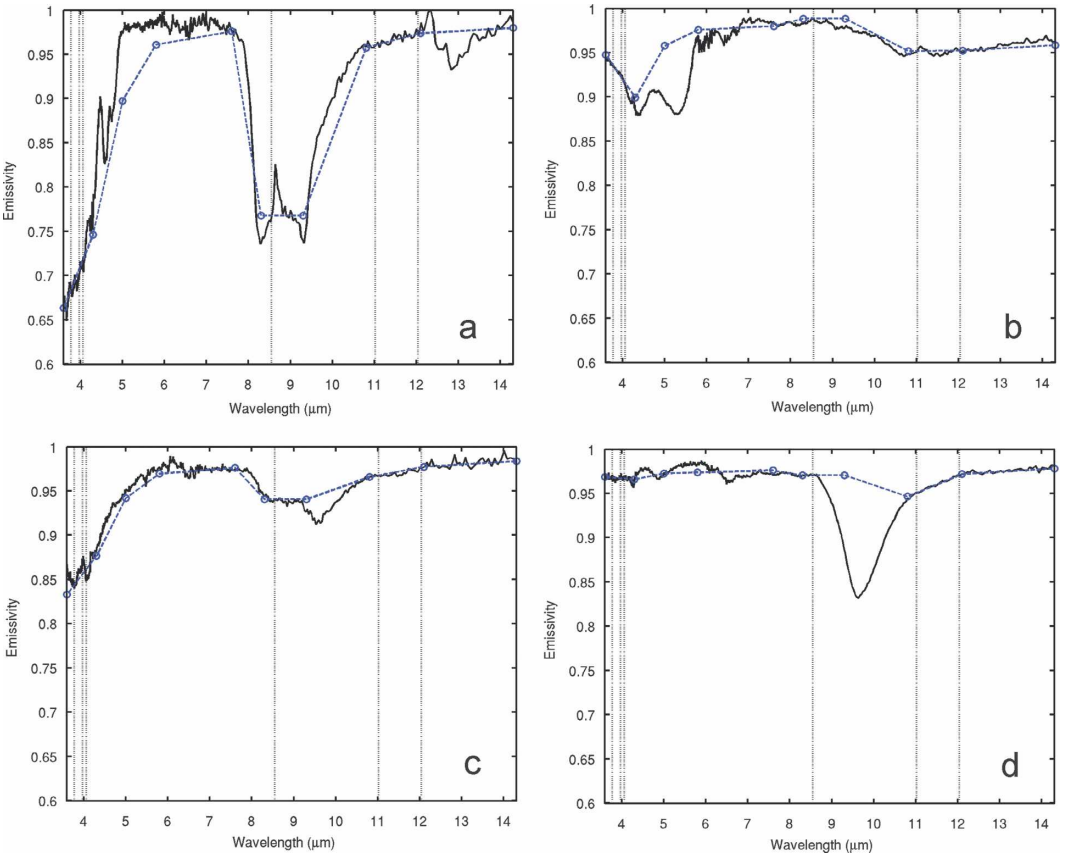

FIG. 6. As in Fig. 5 but spectra are from (a) a soil sample from Page, (b) dry grass, (c) a surface in Death Valley, and (d) a playa surface in Railroad Valley, NV.

sample shows a small emissivity peak near the center of the emission minimum at 8.5 μm. This peak is a common feature associated with the quartz in sandy soils that will not be captured with the resolution of the BF method. Figure 6b also shows the emissivity spectrum for dry grass, which diverges from the BF conceptual model. This spectrum does not begin its rise at 4.3 μm as expected by the BF model but rather remains low until 5.5 μm; therefore, emissivity is overestimated in the 4.3–5.8-μm wavelength range.

Perhaps the most significant limitation of the BF method occurs for materials with a *reststrahlen* feature centered at a higher wavelength than expected by the BF conceptual model. Hunt (1980) and Hook et al. (1998) note that the *reststrahlen* feature occurs at 8.5 μm for quartz and feldspar (framework silicates), but for other types of silicates the feature can occur as high as 12 μm. Figures 6c,d illustrate two surfaces in the ICESS/UCSB database (Railroad Valley and Death Valley, Nevada) for which an emission minimum at higher wavelengths was observed. Both have an emission minimum centered around 9.5 μm that is not captured by the BF method because the only information available is the MOD11 emissivity at 8.5 and 11 μm, and emissivity at these wavelengths remained high.

The combined results of this evaluation for all 123 spectra are presented in Figs. 7 and 8, which show mean absolute difference (fitting error) and standard deviation of the fitting error, respectively, for three approaches: application of the BF method, the assumption of constant emissivity equal to 1.0, and simple linear interpolation between MOD11 wavelengths. The fitting errors for the BF method are never greater than 0.02, and are considerably lower than those for a constant emissivity of 1.0, an assumption still commonly made in many applications. The regions of the most improvement over a constant emissivity of 1.0 are the 3.6–5 and 8–10-μm regions where the actual emissivity can differ greatly from 1.0. The most significant improvements by the BF method over linear interpolation occur in the 4.5–8-μm wavelength region. The standard deviation of the fitting errors is less than 0.03 at all wavelengths except for a peak with standard deviation slightly greater than 0.03 centered around 9.8 μm.

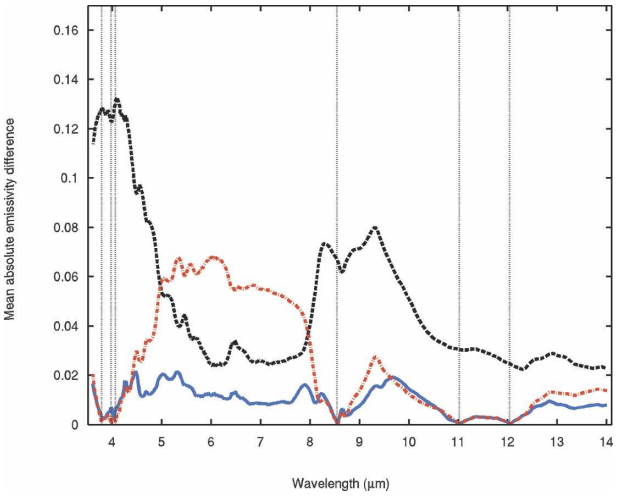

FIG. 7. Mean absolute differences between the 123 ICESS/UCSB original high spectral laboratory emissivity and the derived BF emissivity (blue solid line), a constant emissivity of 1 (black dashed), and emissivity linearly interpolated between the six MOD11 values (red dashed–dotted line). BF emissivity spectra used in this comparison were derived using input at six wavelengths (corresponding to the location of MOD11 emissivity bands, identified by the dotted vertical lines). Results were computed every 5 cm^{-1} wavenumbers.

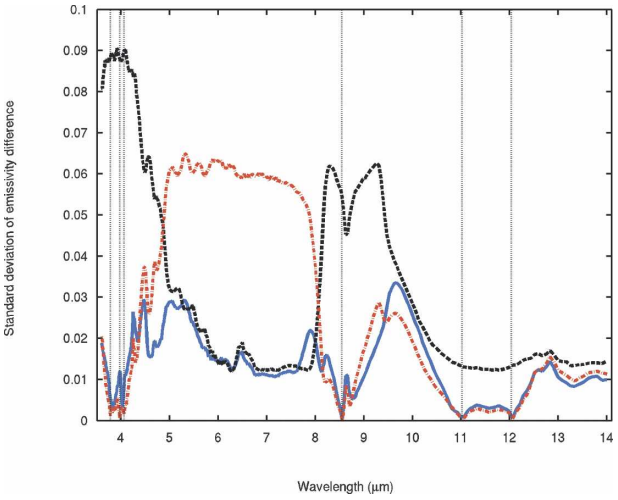

FIG. 8. As in Fig. 7 but for std dev of the differences between the various emissivities and the original high-spectral laboratory emissivity.

The results presented in Figs. 5–8 encompass all wavelengths in the 3.6–14.3-μm range. For MOD07 applications, however, only selected wavelength regions are required. Moreover, the convolution inherent in the MODIS channel spectral response functions (SRFs) averages over any high-spectral-resolution features in the laboratory data. To focus the evaluation on the relevant MODIS bands, the high spectral laboratory measurements and the derived BF spectra (linearly interpolated between hinge points) were first convolved with the MODIS SRF at the 11 MOD07 bands. Results comparing the original laboratory spectra to the BF emissivity at the same MOD07 wavelengths are shown in Table 2. An additional comparison in Table 2 shows the percentage improvement of the BF emissivity spectra over a uniform emissivity of 1.0 (i.e., the reduction in the laboratory–BF differences relative to the laboratory–unity differences). This analysis further indicates that the database is well suited for an application involving multispectral radiances from instruments such as MODIS.

Because the baseline fitting procedure was developed conceptually from examination of the same 123 ICESS/UCSB spectra used for the evaluation in this section, the assessment is not independent. A separate collection of high-spectral-resolution aircraft- or ground-based measurements of actual land surface emissivities over widely varying surface characteristics would be required to accurately evaluate the approach. In the absence of such a dataset, a similar evaluation to that presented in Table 2 was performed for a much larger dataset of 989 spectra of laboratory-measured emissivity using materials from the ASTER spectral library (see Fig. 9). The original ASTER library was screened according to the same criteria used for the ICESS/UCSB spectra outlined in section 3a(1). The BF spectra were derived using input from the laboratory spectra at the six MOD11 wavelengths, and then both laboratory and BF spectra were convolved with the MODIS SRF as described above. The results of this analysis for the 11 MOD07 bands are presented in Table 3. Some of the 989 spectra from the ASTER spectral library are generated from raw minerals and other materials that may exist in combination within soils and rocks, rather than materials that independently compose land surfaces. Hence, their behavior may not be typical of actual land surface conditions, and the results in Table 3 likely overestimate the errors actually present when the BF method is applied to satellite measurements of earth scenes. This analysis confirms the improvement that can be achieved by using the BF emissivity database in an application with multispectral radiances such as MODIS.

4. Application of surface emissivity to training data

The BF procedure can be applied to every latitude–longitude pair for *Terra* MOD11 or *Aqua* MYD11 emissivity data at the granule scale or the level-3 daily,

TABLE 2. Comparison of high-spectral laboratory-measured emissivity with the BF emissivity (derived using input from the corresponding laboratory spectra at the 6 MOD11 wavelengths) for 123 spectra from the ICESS/UCSB emissivity library. Before comparing at MOD07 bands, both the laboratory and the BF (linearly interpolated between hinge points) emissivity were convolved with the MODIS SRF.

MODIS channels used in MOD07	25	27	28	29	30	31	32	33	34	35	36
Wavelength (μm)	4.5	6.7	7.3	8.6	9.7	11.0	12.0	13.3	13.6	13.9	14.2
Mean absolute difference (laboratory − BF)	0.016	0.009	0.009	0.002	0.018	0.001	0.001	0.007	0.008	0.008	0.008
Std dev (laboratory, BF)	0.022	0.013	0.012	0.002	0.032	0.002	0.002	0.009	0.010	0.010	0.010
% improvement in mean absolute difference, BF vs emissivity = 1	83	67	64	98	71	97	95	74	68	67	66

8-day, or monthly averages depending on the time scale required and the significance of continuous (cloud free) data coverage. For application to MOD07 retrievals, BF emissivities were derived from *Aqua* MODIS level-3 monthly averaged MYD11 data from 2004 (similar results were obtained with emissivity derived from 2003 and 2005 MYD11 data). The result is a spectrum of land surface emissivities at 10 hinge-point wavelengths for each MYD11 latitude–longitude pair (0.05° spatial resolution) for each month over land. Because many of the training data profiles are radiosondes with standard launch times that do not match either *Terra* or *Aqua* overpass times globally, the significance of the choice of satellite (*Aqua* or *Terra*) used to derive the BF data for application to MOD07 is minimal.

Seemann et al. (2003) demonstrated that retrievals of total precipitable water (TPW) are improved by partitioning the training data into brightness temperature (BT) classes using MODIS band 31 (11 μm). This partitioning technique has been incorporated into the operational MOD07 algorithm and was used to perform the retrievals presented here.

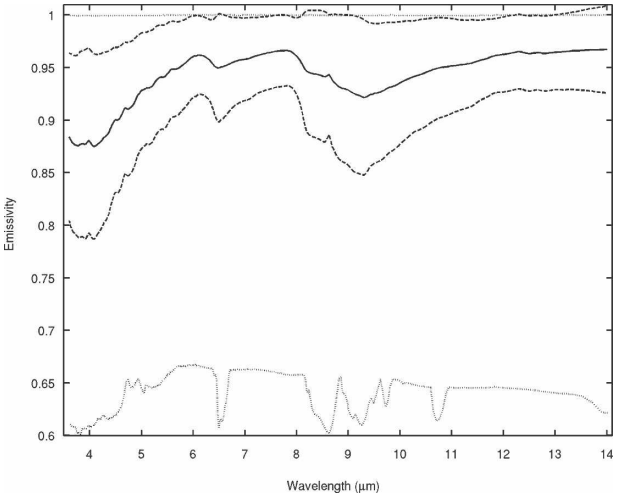

FIG. 9. As in Fig. 2 but for 989 land surface emissivity spectra from the ASTER and ICESS/UCSB spectral libraries.

This section presents results from applying the BF surface emissivity in MOD07 integrated retrieved moisture profiles and details some of the processing considerations.

a. *Filling of data in grid points with no MOD11 input*

The BF approach relies on data from the MOD11 emissivity products, which have known gaps. Even for the level-3 monthly averaged MOD11 emissivity product, there are locations with no data because of the absence of any clear sky MODIS observations in an entire month. Additionally, in the polar regions, certain MOD11 conditions are often not met. The MOD11 day/night algorithm requires that the solar zenith angle is less than 75° for the daytime data and greater than 90° for nighttime data, that day and night data are within 32 days, and that the brightness temperature in band 31 (11 μm) is greater than or equal to 198 K (day) or 195 K (night; Z. Wan 2006, personal communication). For grid points with no MOD11 data available for a given month and latitude–longitude pair, the BF emissivities at the same latitude–longitude for the two adjacent months (preceding and following), if available, are averaged. If emissivity is available for only one of the two adjacent months, that value is used. If there was no input MOD11 data for the 3-month period, then the annual average emissivity for the same latitude–longitude pair is used. In the Antarctic, there are regions where MOD11 data are not available during the course of a whole year, because of the constraint that band 31 brightness temperatures must be greater than 198 K (day) or 195 K (night). In these cases, an average of all emissivity for a given month and a given wavelength from regions with latitude less than −80°S was used to fill the remaining Antarctic data gaps.

Figure 10 shows examples of BF emissivity (with data gaps filled where applicable) for the Sahara Desert region in northern Africa at selected hinge-point wavelengths for August 2003. The high spatial resolution

TABLE 3. As in Table 3 but statistics were computed for 989 spectra from the ASTER and ICESS/UCSB spectral libraries.

MODIS channels used in MOD07	25	27	28	29	30	31	32	33	34	35	36
Wavelength (μm)	4.5	6.7	7.3	8.6	9.7	11.0	12.0	13.3	13.6	13.9	14.2
Mean absolute difference (laboratory − BF)	0.022	0.026	0.021	0.002	0.026	0.002	0.001	0.013	0.013	0.014	0.014
Std dev (laboratory, BF)	0.036	0.041	0.034	0.005	0.045	0.005	0.002	0.021	0.025	0.027	0.029
% improvement in mean absolute difference, BF vs emissivity = 1	76	42	42	96	63	96	97	67	62	59	57

made possible by the use of MODIS MYD11 for input is illustrated by the detail visible in the Nile River and Delta. The transition from arid to semiarid as the Sahara Desert gives way to more vegetation is indicated by the increase in 4.3- and 8.3-μm emissivity toward the south.

b. Impacts of emissivity on TPW retrieval results

A modified version of the MOD07 operational algorithm was used to compute the TPW from MODIS radiance measurements (integrated from retrieved moisture profiles) and examine the impacts of surface emissivity on the retrieval of atmospheric moisture profiles over land. The emissivity assigned to the profiles in the training dataset of the MOD07 retrieval algorithm was varied to include constant surface emissivity values of 1.0, 0.95, and the emissivity derived by the BF approach for the corresponding month and latitude–longitude for each of the 11 MODIS bands used in the MOD07 algorithm. For this comparison, the constant emissivities (0.95 or 1.0) were applied to all training profiles, including those over land and water. The BF emissivity was only assigned to training profiles over land, and profiles over ocean and inland bodies of water were assigned an emissivity using the operational MOD07 emissivity for seawater based on the approach of Wu and Smith (1997).

Comparisons among the TPW retrieved using regression coefficients computed with the various emissivities are presented in this section. Comparisons with products derived from other ground- and satellite-based sensors are also included for validation of the retrievals performed with the BF emissivity.

1) TPW AT THE ARM SGP SITE IN OKLAHOMA

TPW retrievals from *Terra* MODIS IR radiances were performed for a collection of 312 clear sky cases from April 2001 to August 2005 at the Atmospheric Radiation Measurement (ARM) (Stokes and Schwartz 1994; Ackerman and Stokes 2003) Southern Great Plains (SGP) site in Lamont, Oklahoma. These cases were selected by manual inspection of MODIS visible and IR radiance imagery to avoid cloudy scenes without relying solely on the MODIS operational cloud mask product that is used in the MOD07 algorithm. The retrievals were performed using coefficients derived with various emissivities. The difference between TPW computed with an emissivity of 1.0 and TPW computed using the BF emissivity is shown in Fig. 11. A general increase in TPW (up to 8 mm for some of the moist cases) is observed with the BF emissivity compared to an emissivity of 1.0.

In general, if the assumed surface emissivity included in the training dataset is higher than the true state, then the corresponding calculated radiances will be high. To compensate for the differences between the calculated and observed radiances, the retrieved profile based on the observed radiances will be cooler in temperature or lower in moisture than the actual state. Based on this logic, and assuming true emissivity is generally less than 1.0, retrievals of TPW made with coefficients derived using a constant emissivity of 1.0 assigned to the training data profiles are expected to be drier than those derived using the BF emissivity. Figure 11 is consistent with this prediction. However, the difference between TPW retrieved with an emissivity of 1.0 and TPW retrieved with the BF emissivity is not always negative, because both temperature and water vapor of the retrieval can react simultaneously to compensate for the reduction of surface emissivity. In addition, the retrieval can become unphysical and unstable if the training database includes an emissivity that cannot sufficiently account for the compensation induced by the individual retrieval variable such as temperature or water vapor.

To examine whether the higher TPW retrieved with the BF emissivity is more accurate than TPW retrieved with the commonly assumed uniform emissivity of 1.0, MODIS TPW retrievals for these 312 clear sky cases at the ARM SGP site are compared in Figs. 12a,b to measurements obtained using ground-based microwave radiometer (MWR; Westwater 1993; Liljegren and Lesht 1996). For reference, TPW retrievals using the *GOES-8*

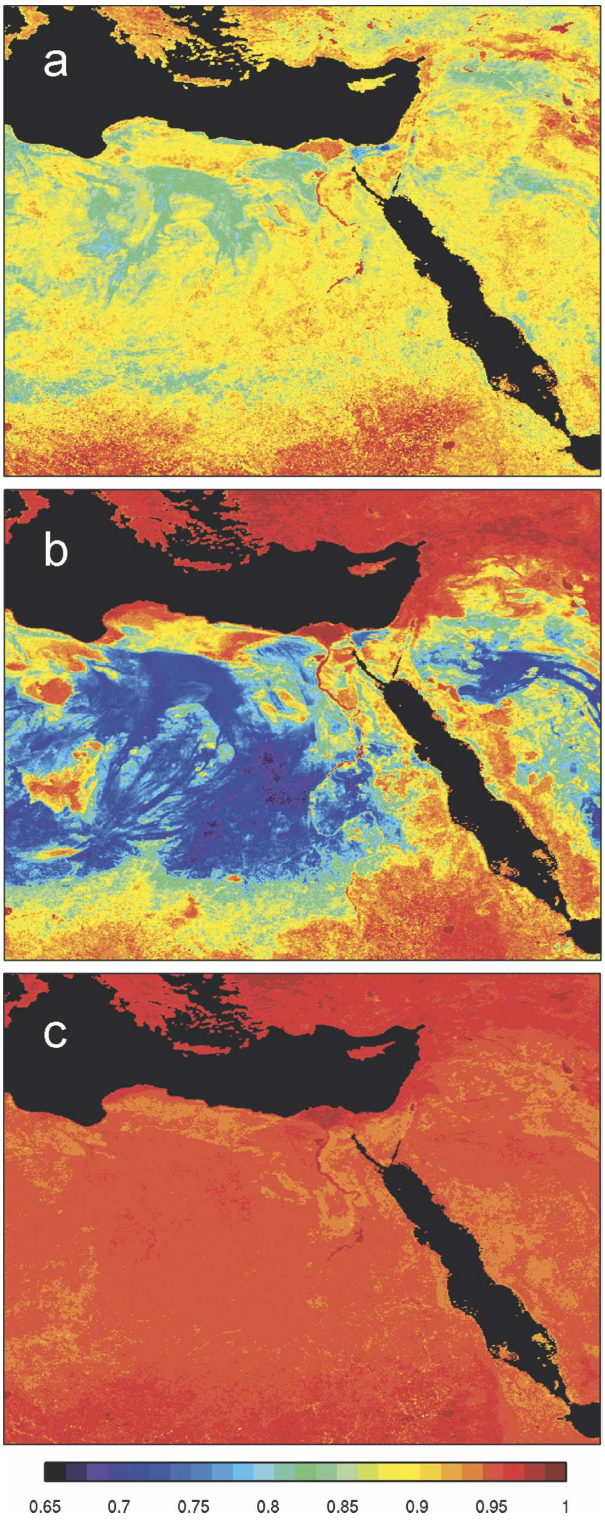

FIG. 10. Surface emissivity derived from the BF approach for August 2003 in the eastern Sahara Desert region. Emissivity is shown for three wavelengths: (a) 4.3, (b) 8.3, and (c) 10.8 μm. The Nile River can be seen curving south from its delta, as identified by the high emissivity characteristic of water.

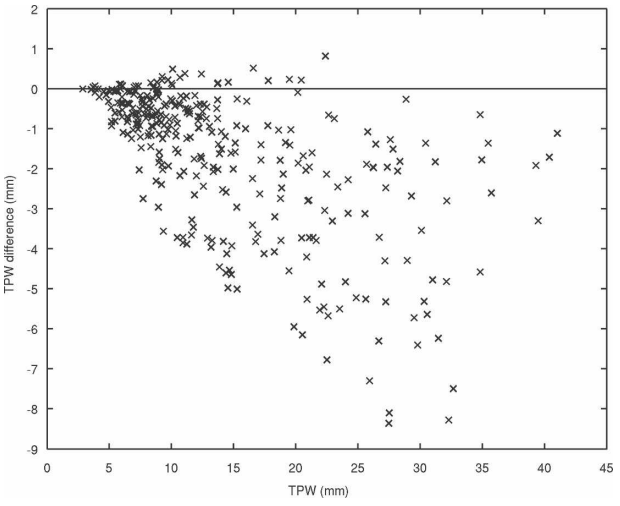

FIG. 11. Difference (mm) between TPW retrieved from a training dataset with a constant surface emissivity of 1.0 minus that retrieved with the BF emissivity. Retrievals were performed using *Terra* MODIS radiances for 312 clear sky cases at the ARM SGP site between April 2001 and August 2005.

and *-12* sounding instruments and TPW measurements obtained from radiosondes launched at the ARM SGP site are also compared with MWR measurements in Fig. 12. The same cases were evaluated for each instrument; however, GOES data were frequently missing (because of cloud-mask differences or data outages), so only 169 GOES cases are included in the comparison. For the radiosondes, the 280 cases shown were measured within 2 h of the *Terra* MODIS overpass time. Table 4 summarizes statistics from this comparison and for retrievals made with various other emissivities.

Figure 12 and Table 4 demonstrate that BF emissivity-based TPW retrievals at the ARM SGP site agree better with the TPW values measured by ground-based instruments (radiosondes and microwave water radiometer) and TPW retrievals from other satellite-based (*GOES-8* and *-12*) data than the uniform emissivity-based TPW retrievals. The root-mean-square error (RMSE) between the MWR and MODIS TPW computed with a constant emissivity of 1.0 is 3.8 mm, as compared with 2.5 mm for TPW computed with the BF emissivity. With the constant emissivity of 1.0, MODIS TPW is too low for moist cases (TPW $>$ 10 mm), with an average bias over all cases (MWR minus MODIS) of 1.9 mm. With the BF emissivity, the dry bias is reduced to 0.2 mm. The dry bias is even more pronounced if the retrievals are performed using a constant emissivity of 0.95, for which the bias is 2.1 mm and the RMSE is 4.3 mm. If the emissivity model used for NOAA-88 training data in the original MODIS and ATOVS algorithms (see section 2a; Fig. 1) is applied to all the training

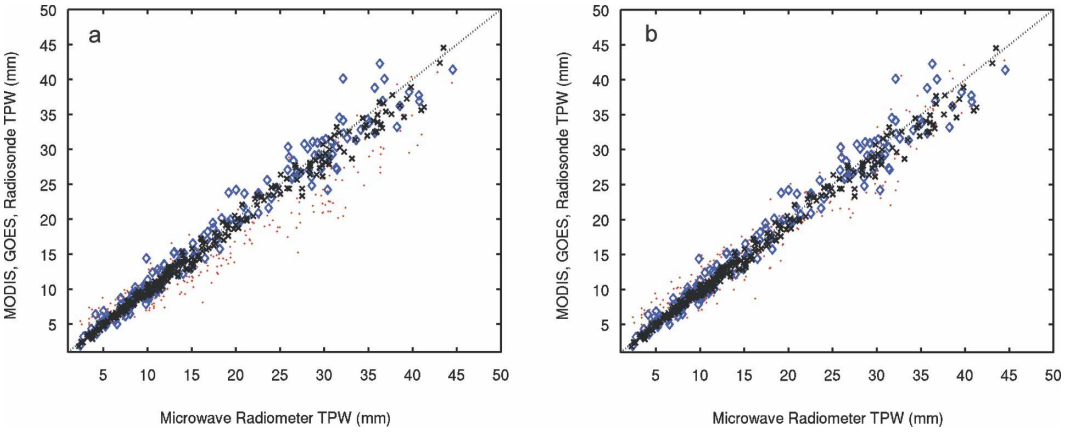

FIG. 12. Comparison of total precipitable water (mm) at the ARM SGP site from *Terra* MODIS (red dots), *GOES-8* and *-12* (blue diamonds), and radiosonde (black x), all on the *y* axis with the ground-based ARM SGP microwave water radiometer (*x* axis) for 312 clear sky cases from April 2001 to August 2005. (a) A constant emissivity of 1.0 was used in the training data of the MODIS retrievals and (b) the BF emissivity presented in this paper was used. The dotted diagonal line indicates a 1:1 agreement between the MWR and satellite or radiosondes TPW.

profiles, the result is only slightly better than that for a constant emissivity of 1.0 (RMSE compared with the MWR is 3.5 mm and bias is 1.6 mm).

2) TPW FOR THE SAHARA DESERT

The TPW sensitivity presented in Figs. 11 and 12 represents the behavior of only a single geographical region. The retrieval error characteristics (bias and variance) depend on the amplitude and spectral structure of the surface type for which retrievals are performed. Therefore, if a sensitivity analysis is performed for other global land surfaces, different behavior for different land surface types is observed, with the most significant effects of a change in emissivity occurring in desert and semiarid regions. An assumption of constant emissivity for a desert case will result in larger retrieval errors than for other land surface types due to the large spectral structure inherent in the actual surface emissivity of sandy soil, specifically the very low emission at 4 and 8.5 μm characteristic of the quartz minerals that compose most sandy soils.

Figure 13 presents a comparison of the TPW retrievals made with two different emissivities in the Sahara Desert of northern Africa for *Aqua* ascending (local night) passes on 1 August 2005, along with the analysis from the National Centers for Environmental Prediction (NCEP) Global Data Assimilation System (GDAS). The GDAS analysis includes TPW for both clear and cloudy areas, while MODIS is a clear sky algorithm, so GDAS shows high TPW in the cloudy areas south of the Sahara Desert where MODIS has no retrievals. When a constant emissivity of 0.95 is used for all bands and profiles (Fig. 13a), very high TPW values (up to 110 mm) with considerable noise are retrieved in this typically dry desert area. This retrieval instability occurs because the regression has not been sufficiently trained by realistic surface and atmospheric conditions. When the BF emissivity is assigned to the profiles in the training data (Fig. 13b), the TPW agrees much better with the GDAS analysis (Fig. 13c).

Figure 14 presents a closer look at one 5-min *Terra* MODIS granule from the north-central Sahara Desert for 2140 UTC of the same day shown in Fig. 13. TPW in Fig. 14 was retrieved using constant emissivities of 0.95, 1.0, and the BF emissivity. The TPW retrievals made using the BF emissivity (Fig. 14c) agree with the NCEP GDAS TPW (Fig. 13c) better than those made with a constant emissivity of either 0.95 or 1.0 (Figs. 14a,c, respectively). For this case, the TPW retrieved with an

TABLE 4. RMSE, bias, and number of cases for a comparison between the MWR TPW measured at the ARM SGP site and that from *Terra* MOD07, *GOES-8* and *-12*, and radiosondes for clear sky cases between April 2001 and August 2005. MOD07 results are presented for four different emissivities applied to the training data profiles used in retrieving the TPW.

	RMSE (mm)	Avg bias (MWR − other) (mm)	*N*
MOD07, BF emissivity	2.5	0.2	312
MOD07, emissivity = 1.0	3.8	1.9	312
MOD07, emissivity = 0.95	4.3	2.1	312
MOD07, NOAA-88 emissivity	3.6	1.6	312
GOES-8 and *-12*	2.9	0.0	169
Radiosonde	1.2	0.5	280

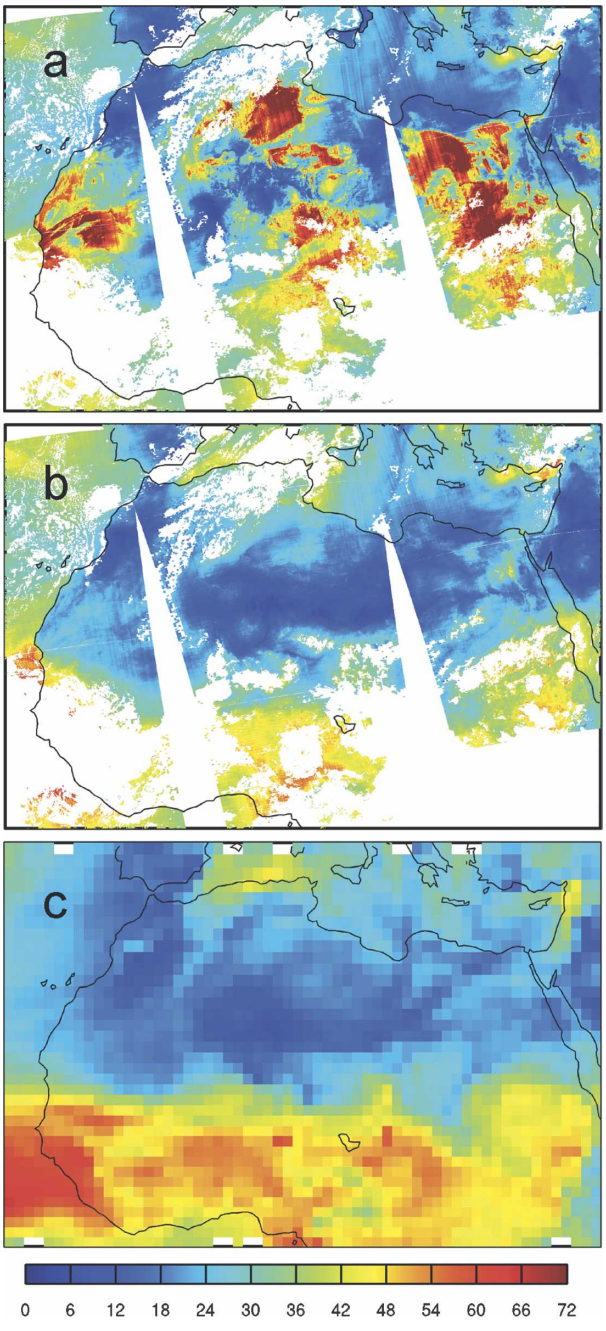

FIG. 13. Images of TPW data (mm) in MOD07 retrieved by two approaches with different surface emissivity used in the training data: (a) emissivity = 0.95 and (b) BF emissivity for all *Terra* MODIS ascending (nighttime) passes over the Sahara Desert region of Africa on 1 Aug 2005. MODIS overpass times range from 2000:00 (eastern Sahara) to 2300:20 UTC (western Sahara). (c) For comparison, the 0000 UTC NCEP GDAS TPW analysis from 2 Aug 2005 is shown. The white areas in the MODIS image indicate no retrievals because of either cloudy skies or no MODIS data coverage.

emissivity of 1.0 is more reasonable than the TPW retrieved with an emissivity of 0.95. However, there are regions of artificially elevated TPW in retrievals made using both constant emissivity values (1.0 and 0.95) because of retrieval instability resulting from an inaccurate characterization of the surface.

5. Conclusions

A high-spatial- and moderate-spectral-resolution global database of land surface emissivity was developed using a procedure termed the baseline fit method that adjusts a baseline emissivity spectrum based on MOD11 land surface emissivity measurements according to a conceptual model of land surface emissivity. The BF emissivity is derived at 10 hinge points between 3.6 and 14.3 μm, and the result can be linearly interpolated between hinge points for applications requiring a moderate spectral resolution emissivity. The BES, the conceptual model, and the BF procedure to fit the BES to MOD11 measurements were derived with the use of high-spectral laboratory measurements of surface emissivity drawn from a wide range of materials present on the earth's surface. The database was developed for application to clear sky sounding retrievals from multispectral satellite radiance measurements and was applied in this paper to the MOD07 atmospheric profile retrieval algorithm. The potential exists for other applications of the BF database.

The BF database derived from *Aqua* MYD11 data is available online (see http://cimss.ssec.wisc.edu/iremis/). This database has 0.05° spatial resolution and is currently available monthly for 3 yr. The same approach can be applied to MOD11 8-day, daily, or granule-scale data resulting in higher temporal resolution; however, significant reduction in MOD11 data coverage occurs with a shorter averaging period due to the presence of cloudy pixels. For high-spectral applications such as AIRS and GIFTS, the spectral resolution of the BF database will not be sufficient and a different approach for deriving emissivity is needed. Some approaches that may be suitable for the derivation of a high-spectral database of emissivity have been introduced by Borbas et al. (2007) and Zhou et al. (2006).

The ability of the BF method to fill in the spectral gaps between MOD11 measurements was evaluated by applying it to high-spectral laboratory data sampled at only the six MOD11 wavelengths. Linearly interpolating the BF spectra between the 10 hinge points and comparing the results with the original laboratory spectra from the ASTER and ICESS/UCSB databases showed that the BF spectra generally describe the overall spectral shape well but lack the high-spectral fluctuations that cannot be captured with this approach.

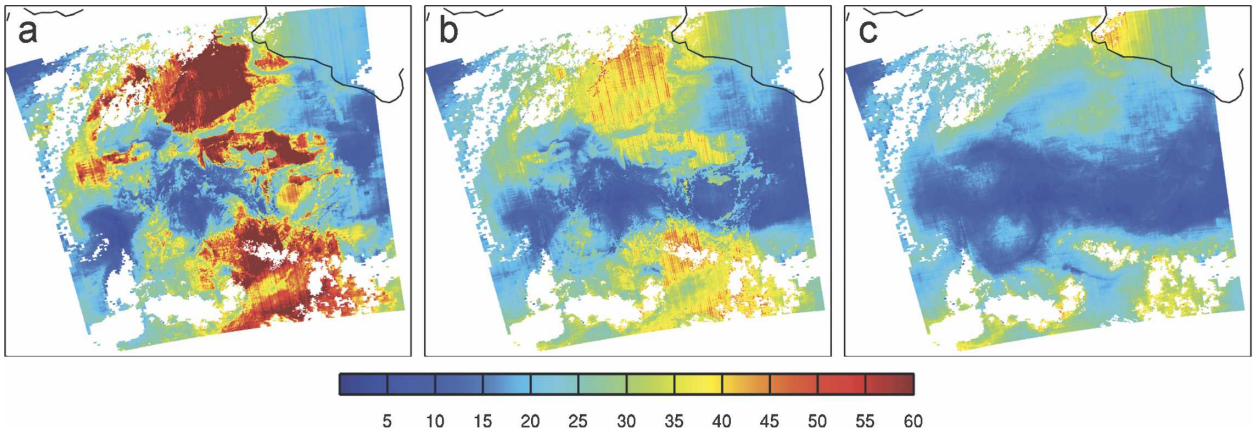

FIG. 14. MOD07 TPW (mm) for the 5-min *Terra* granule beginning at 2100:40 UTC 1 Aug 2005. This granule is in the north-central Sahara Desert and is also shown in Fig. 13, although the color scale range is different. Emissivities of (a) 0.95, (b) 1.0, and (c) the baseline fit emissivity were applied to the training data used in the regression retrieval algorithm.

For multispectral instruments such as MODIS that average over the high-spectral features with filter functions, the piecewise linear representation of the BF emissivity is sufficient.

The evaluation of the BF method presented here measures its ability to fill in the gaps in emissivity measurements between MOD11 values; it does not assess the accuracy of the MOD11 emissivity values assigned at the six MOD11 wavelengths. The accuracy of the BF emissivity database depends on accurate input from MOD11, so any errors in the MOD11 surface emissivity product will be reflected in the database as well [see Wan et al. (2004) for MOD11 validation]. Efforts to assess the validity of the BF product relative to other ground- and satellite-based measurements of emissivity are underway (Moy et al. 2006) and any future global validation work should provide valuable information for further improving the BF method. In addition, as updates to the MOD11 algorithm are made, the BF database will be reprocessed and any improvements in the accuracy of the MOD11 emissivity product will be translated to the BF database.

Evaluation of the emissivity database presented in this paper involved evaluating the impacts of applying the BF emissivity to integrated retrievals of atmospheric moisture profiles in the MOD07 algorithm. Improvements were demonstrated with the new emissivity through comparisons with NCEP GDAS over the Sahara Desert and with the MWR, GOES, and radiosondes at the ARM SGP site. Desert retrievals of TPW made using coefficients derived with the BF emissivity compared well to the NCEP GDAS product, while those made with a uniform emissivity of 1.0 or 0.95 exhibited noisy and unreasonably high TPW values. At the SGP ARM site, the RMSE for TPW as compared with that measured by the MWR was reduced to 2.5 mm by including the BF emissivity in the training data used to compute the coefficients. The average bias (MWR − MODIS) was reduced to 0.2 mm. When retrievals were performed using training data with a constant emissivity of 1.0 and 0.95, the RMSEs were 3.8 and 4.3 mm, and biases were 1.9 and 2.1 mm, respectively.

Acknowledgments. This research was supported by the EOS NASA Grant NNG04HZ39C, NOAA Cooperative Agreement Grant NA06NES4400002, and DOD Navy MURI Grant N00014-01-1-0850. We gratefully acknowledge Zhengming Wan of UCSB for providing the library of laboratory emissivity spectra and helpful discussions. We express our appreciation for the contributions of three anonymous reviewers whose suggestions improved the paper. We also thank Hank Seemann for his thorough editing of the text and Bill Wetzel for helpful assistance in the preparation of final figures. Some laboratory data were obtained through the ASTER spectral library through the courtesy of the Jet Propulsion Laboratory, California Institute of Technology, Pasadena, California. ARM data were obtained from the Atmospheric Radiation Measurement Program sponsored by the U.S. Department of Energy.

REFERENCES

Ackerman, T., and G. Stokes, 2003: The Atmospheric Radiation Measurement Program. *Phys. Today,* **56,** 38–45.

Borbas, E., S. W. Seemann, H.-L. Huang, J. Li, and W. P. Menzel, 2005: Global profile training database for satellite regression retrievals with estimates of skin temperature and emissivity. *Proc. Int. ATOVS Study Conf. XIV,* Beijing, China, CIMSS/University of Wisconsin—Madison, 763–770. [Available online at http://cimss.ssec.wisc.edu/itwg/itsc/itsc14/proceedings/2_9_Borbas.pdf.]

——, and Coauthors, 2007: A global infrared land surface emissivity database and its validation. Preprints, *11th Symp. on Integrated Observing and Assimilation Systems for the Atmosphere, Oceans, and Land Surface*, San Antonio, TX, Amer. Meteor. Soc., P2.7.

Chedin, A., N. A. Scott, C. Wahiche, and P. Moulinier, 1985: The improved initialization inversion method: A high resolution physical method for temperature retrievals from satellites of the TIROS-N series. *J. Climate Appl. Meteor.,* **24,** 128–143.

Chevallier, F., 2001: Sampled databases of 60-level atmospheric profiles from the ECMWF analyses. Numerical Weather Prediction Satellite Application Facility Research Rep. 4, 28 pp.

Dozier, J., and Z. Wan, 1994: Development of practical multiband algorithms for estimating land-surface temperature from EOS/MODIS data. *Adv. Space Res.,* **14** (3), 81–90.

Gillespie, A., S. Rokugawa, S. Hook, T. Matsunaga, and A. Kahle, 1999: Temperature/emissivity separation algorithm theoretical basis document, version 2.4. NASA Contract NAS5-31372, 64 pp. [Available online at http://eospso.gsfc.nasa.gov/eos_homepage/for_scientists/atbd/docs/ASTER/atbd-ast-05-08.pdf.]

Hayden, C. M., 1988: GOES-VAS simultaneous temperature-moisture retrieval algorithm. *J. Appl. Meteor.,* **27,** 705–733.

Hook, S. J., T. J. Cudahy, A. B. Kahle, and L. B. Whitbourn, 1998: Synergy of active and passive airborne thermal infrared systems for surface compositional mapping. *J. Geophys. Res.,* **103** (B8), 18 269–18 276.

——, W. B. Clodius, L. Balick, R. E. Alley, A. Abtahi, R. C. Richards, and S. G. Schladow, 2005: In-flight validation of mid and thermal infrared data from the Multispectral Thermal Imager (MTI) using an automated high altitude validation site at Lake Tahoe CA/NV, USA. *IEEE Trans. Geosci. Remote Sens.,* **43,** 1991–1999.

Hunt, G. R., 1980: Electromagnetic radiation: The communication link in remote sensing. *Remote Sensing in Geology,* B. S. Siegal and A. R. Gillespie, Eds., John Wiley and Sons, 5–45.

Kleespies, T. J., P. van Delst, L. M. McMillin, and J. Derber, 2004: Atmospheric transmittance of an absorbing gas. 6. OPTRAN status report and introduction to the NESDIS/NCEP Community Radiative Transfer Model. *Appl. Opt.,* **43,** 3103–3109.

Knuteson, R., F. Best, D. DeSlover, B. Osborne, H. Revercomb, and W. Smith Sr., 2004: Infrared land surface remote sensing using high spectral resolution aircraft observations. *Adv. Space Res.,* **33,** 1114–1119.

Korb, A. R., P. Dybwad, W. Wadsworth, and J. W. Salisbury, 1996: Portable Fourier transform infrared spectroradiometer for field measurement of radiance and emissivity. *Appl. Opt.,* **35,** 1679–1692.

Kornfield, J., and J. Susskind, 1977: On the effect of surface emissivity on temperature retrievals. *Mon. Wea. Rev.,* **105,** 1605–1608.

Li, J., W. Wolf, W. P. Menzel, W. Zhang, H.-L. Huang, and T. H. Achtor, 2000: Global soundings of the atmosphere from ATOVS measurements: The algorithm and validation. *J. Appl. Meteor.,* **39,** 1248–1268.

Liljegren, J. C., and B. M. Lesht, 1996: Measurements of integrated water vapor and cloud liquid water from microwave radiometers at the DOE ARM cloud and radiation testbed in the US Southern Great Plains. *Proc. Int. Geoscience and Remote Sensing Symp.,* Lincoln, NE, IEEE, 1675–1677.

Moy, L., E. Borbas, S. Seemann, H.-L. Huang, R. Knuteson, I. Trigo, and L. Zhou, 2006: Comparison of land surface infrared emissivity from MODIS, AIRS, and SEVIRI. *Eos, Trans. Amer. Geophys. Union,* **87** (Fall Meeting Suppl.), Abstract A21D-0850.

Ogawa, K., and T. Schmugge, 2004: Mapping surface broadband emissivity of the Sahara desert using ASTER and MODIS data. *Earth Interactions,* **8.** [Available online at http://EarthInteractions.org.]

Prabhakara, C., and G. Dalu, 1976: Remote sensing of the surface emissivity at 9 μm over the globe. *J. Geophys. Res.,* **81,** 3719–3724.

Salisbury, J. W., and D. M. D'Aria, 1992: Emissivity of terrestrial materials in the 8-14 μm atmospheric window. *Remote Sens. Environ.,* **42,** 83–106.

——, and ——, 1994: Emissivity of terrestrial materials in the 3-5 μm atmospheric window. *Remote Sens. Environ.,* **47,** 345–361.

——, A. Wald, and D. M. D'Aria, 1994: Thermal-infrared remote sensing and Kirchhoff's law 1. Laboratory measurements. *J. Geophys. Res.,* **99,** 11 897–11 911.

Schmugge, S., J. Hook, and C. Coll, 1998: Recovering surface temperature and emissivity from thermal infrared multispectral data. *Remote Sens. Environ.,* **65** (2), 121–131.

Seemann, S. W., J. Li, W. P. Menzel, and L. E. Gumley, 2003: Operational retrieval of atmospheric temperature, moisture, and ozone from MODIS infrared radiances. *J. Appl. Meteor.,* **42,** 1072–1091.

——, E. Borbas, J. Li, W. P. Menzel, and L. E. Gumley, cited 2006: MODIS atmospheric profile retrieval algorithm theoretical basis document. [Available online at http://modis.gsfc.nasa.gov/data/atbd/atbd_mod07.pdf or http://modis.gsfc.nasa.gov/data/atbd/atmos_atbd.php.]

Snyder, W., and Z. Wan, 1998: BRDF models to predict spectral reflectance and emissivity in the infrared. *IEEE Trans. Geosci. Remote Sens.,* **36,** 214–225.

Stokes, G. M., and S. E. Schwartz, 1994: The Atmospheric Radiation Measurement (ARM) program: Programmatic background and design of the cloud and radiation testbed. *Bull. Amer. Meteor. Soc.,* **75,** 1201–1221.

Wan, Z., 1999: MODIS land-surface temperature algorithm theoretical basis document (LST ATBD). Tech. Rep. version 3.3, Institute for Computational Earth System Science, University of California, Santa Barbara, 77 pp. [Available online at http://modis.gsfc.nasa.gov/data/atbd/atbd_mod11.pdf.]

——, and Z.-L. Li, 1997: A physics-based algorithm for retrieving land-surface emissivity and temperature from EOS/MODIS data. *IEEE Trans. Geosci. Remote Sens.,* **35,** 980–996.

——, Y. Zhang, Q. Zhang, and Z.-L. Li, 2004: Quality assessment and validation of the MODIS global land surface temperature. *Int. J. Remote Sens.,* **25,** 261–274.

Westwater, E. R., 1993: Ground-based microwave remote sensing of meteorological variables. *Atmospheric Remote Sensing by Microwave Radiometry,* M. A. Jensen, Ed., Wiley, 145–213.

Wu, X., and W. L. Smith, 1997: Emissivity of rough sea surface for 8-13 μm: Modeling and verification. *Appl. Opt.,* **36,** 2609–2619.

Zhou, D. K., A. M. Larar, W. L. Smith, and X. Liu, 2006: Surface emissivity effects on thermodynamic retrieval of IR spectral radiance. *Multispectral, Hyperspectral, and Ultraspectral Remote Sensing Technology, Techniques, and Applications,* W. L. Smith Sr. et al., Eds., International Society for Optical Engineering (SPIE Proceedings Vol. 6405), doi:10.1117/12.694283.

Zhou, L., R. E. Dickinson, Y. Tian, M. Jin, K. Ogawa, H. Yu, and T. Schmugge, 2003: A sensitivity study of climate and energy balance simulations with use of satellite derived emissivity data over Northern Africa and the Arabian Peninsula. *J. Geophys. Res.,* **108,** 4795, doi:10.1029/2003JD004083.